

# A Low-Cost Capacitive Relative Humidity Sensor for Food Moisture Monitoring Application

Bo WANG<sup>1</sup>, Man Kay LAW<sup>2</sup> and Amine BERMAK<sup>1</sup>

<sup>1</sup>ECE Department, Hong Kong University of Science and Technology, Clear Water Bay, Kowloon, Hong Kong SAR

<sup>2</sup>The State Key Laboratory of Analog and Mixed-Signal VLSI, University of Macau, Macao, China

Emails: vandy@ust.hk, mklaw@umac.mo, eebermak@ust.hk

**Abstract**—In this paper, a low-cost capacitive relative humidity hygrometer suitable for food moisture monitoring is presented. The variation of dielectric constant of polyimide film to relative humidity enables the sensor's functionality. A fully differential capacitance to digital converter is utilized as the hygrometer digital readout, which is immune to circuit wiring parasitic and enable the sensor's long-term stability. The humidity sensor is implemented using TSMC1P6M 0.18 $\mu$ m technology with thick top metal option. Simulation results indicate that an inaccuracy of  $\pm 6\%$  RH can be achieved sensing from 10% RH  $\sim$  90% RH, with 5.4 $\mu$ W power consumption for sensing and 21.6mW power consumption for sensor heating .

## I. INTRODUCTION

Relative humidity monitoring and control gain rapidly increasing applications in the field of hazardous environment monitoring, weather forecasting, pharmacy production, store etc. Especially in food monitoring applications, hygrometer working together with a temperature sensor becomes more attractive. With the possibility of integrating humidity sensor and temperature sensor on the same substrate, sensing-system-on-chip (SSOC) can be achieved. However, SSOC requires CMOS compatible humidity sensor that has digital output capability for fast data processing.

Several humidity sensor system with different sensing mechanisms have been reported. Gioglio et. al. [1] fully characterized the a.c. electrical characterization of a humidity sensor based on a ceramic material, anodic aluminum oxide ( $\text{Al}_2\text{O}_3$ ). It was revealed that  $\text{Al}_2\text{O}_3$  can measure very low relative humidity for its small pore radius. Afterwards, Cheng et. al. [2] developed a highly sensitive relative humidity sensor using amorphous  $\text{Al}_2\text{O}_3$  nanotubes, which exhibits high sensitivity and fast response at low RH. However, for  $\text{Al}_2\text{O}_3$ , when exposed for a long time in high humidity, significant degradation in the sensitivity and drift in the capacitance characteristics would deteriorate its performance[3]. Semiconductor-material-based humidity sensors, like stannic oxide ( $\text{SnO}_2$ ), also exhibit high linearity and fast response[4], while their reduced sensing range, poor temperature stability and high manufacturing become the bottlenecks[3]. Recently, Seok-Ho Song et. al. [5] developed a MOSFET based relative humidity sensor without using other specific sensing materials. It utilizes the phenomenon that the gate charge dissipation rate through the silicon dioxide varies with ambient relative humidity, which is low-cost and highly CMOS compatible. However, the response is extremely slow at low RH (eg. 3650s

at 19%RH), and the sensor performance is highly process dependant since it depends on the FET's RC constant.

Besides the above mentioned sensing mechanisms, polymer has been widely adopted for relative humidity sensing, whose dielectric constant or conductance varies with ambient relative humidity, corresponding to capacitive type or resistive type sensor. Most of the existing works [6][7][8] utilize the capacitive characteristic of polymer for humidity sensing for its more linear humidity response. Moreover, capacitive sensors are usable over the entire range of 0~100% relative humidity, comparing with 20%~90% range of resistive ones. In this work, polyimide (kapton) is selected as the sensing material. For polyimide, the concentration of absorbed water was found to depend only on the relative humidity and not on the temperature or polymer thickness [9]. As a consequence, the change of the dielectric constant is solely induced by water absorption, thus becomes an excellent indication of the ambient relative humidity. Meanwhile, polyimide coating can be accomplished together with the CMOS circuit fabrication in the foundry instead of laborious post-manufacturing, which can significantly reduce the unit sensor cost.

In this work, a polyimide-based humidity sensor is presented, together with a fully differential capacitance to digital converter (CDC) for digital readout. The designed converter is immune to circuit wiring parasitic and the ratio-metric readout ensures the relative humidity sensor's long-term stability. The sensor is designed in TSMC 0.18 $\mu$ m 1P6M mixed signal process with thick metal option. Simulation results indicate the designed sensor has the capability of 10%  $\sim$  90% relative humidity range sensing with  $\pm 6\%$  RH sensing inaccuracy after output linearization. The sensor consumes 5.4 $\mu$ W power for humidity sensor readout and 21.6mW power for front-end heating, respectively.

## II. RELATIVE HUMIDITY SENSING PRINCIPLE

Relative humidity is defined as the ratio of the partial pressure of water vapor to the saturated vapor pressure of water at a prescribed temperature. As stated above, the weight of water absorbed between the polymeric molecules free space is proportional to relative humidity, which will change the dielectric constant of the polyimide. Though has been thoroughly investigated for relative humidity sensing, basic sensing principles of polyimide need still to be stated. Meanwhile, a various of sensing error sources have to be taken into

consideration for the sensor front-end.

### A. Relative Humidity Sensor Front-end Structure

For CMOS process, interdigitated top metal fingers, with polyimide filled into the finger gaps, can be utilized for capacitive humidity sensing. The line-to-line coupling capacitance of the top metal are sensitive to the dielectric constant of the filling material. Meanwhile, benefit from the high precision of photolithography, such kind of sensing structure is highly reproducible with less inter-die variations. Fig.1 shows the relative humidity sensor front-end structure, along with its associated capacitors.

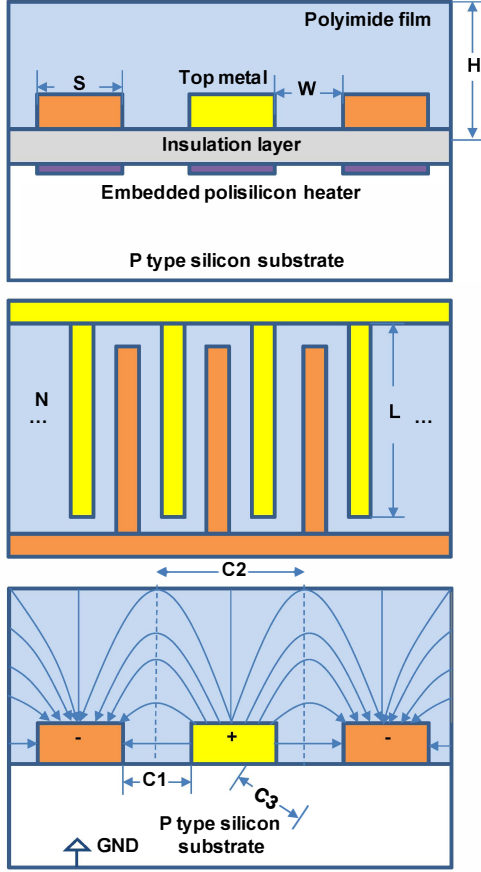


Fig. 1. Humidity sensor front-end structure (top); Top view of the designed interdigitated top metal fingers (middle); Capacitance distribution of the front-end structure (below): C1-top metal line-to-line capacitance. C2-Parasitic capacitance between top metal and polyimide; C3-capacitance between top metal and substrate;

For the sensor front-end, the top metal width is  $S$ , metal-to-metal gap is  $W$ , finger length is  $L$ . And the deposited polyimide film thickness is  $H$ , which is generally larger than metal thickness  $h$ . For TSMC 0.18 $\mu\text{m}$  technology, the typical thickness of top metal M6 is 9900 $\text{\AA}$ . In order to increase front-end capacitance sensitivity and minimize the required chip area, width between top metal fingers is designed to be 2.5 $\mu\text{m}$ , which is the minimum pitch of this process[10].

As shown in Fig.1, the capacitive front-end consists of three main capacitance: top metal line-to-line capacitance  $C1$ ,

parasitic capacitance between top metal and polyimide  $C2$  and parasitic capacitance between top metal and the substrate  $C3$ . The absolute capacitance of the front-end are not only sensitive to ambient relative humidity but to circuit wiring parasitic and fabrication process, including dielectric layer thickness, metal thickness etc. Specific readout design is therefore required to get rid of these influences. In this work, a fully differential capacitance readout scheme is adopted [11], which converts only the capacitance change instead of absolute capacitance into digital reading, as shown in section II-C. Moreover, in order to reduce the sensing hysteresis[12], a polysilicon heater is embedded underneath the interdigitated metal lines as shown in Fig.1. Since polysilicon has a low thermal constant, during sensing, all the metal fingers are guaranteed to operate at the same temperature. Resistance of the polysilicon in this design is 150 ohm, draw a power of 21.6mW with 1.8V supply.

### B. Sensing Front-end Modeling and Analysis

Since the relative humidity sensor front-end can not be simulated directly, preliminary design verification is conducted by front-end modeling. Several capacitive models for interdigitated structures exist that have sufficient agreement between the model and the real device behavior, which share common algorithms like partial capacitance technique or finite element method (FEM) [13][14][15]. A well-known semi-empirical equation describing the dielectric constant of a humid polyimide by Looyenga is given in (1) [10]:

$$\varepsilon_{Mix} = [\gamma \cdot (\varepsilon_{H_2O}^{\frac{1}{3}} - \varepsilon_{Poly}^{\frac{1}{3}}) + \varepsilon_{Poly}^{\frac{1}{3}}]^3 \quad (1)$$

where  $\gamma$  is the fractional volume of water absorbed in polyimide, whose relationship with relative humidity can be modeled by Daubinin equation (2) [10], and other symbol explanations are listed below:

$$\gamma = \gamma_m \phi(T) RH^{\beta(T)} \quad (2)$$

- $\varepsilon_{Mix}$ : dielectric constant of polyimide mixed with water molecular;
- $\varepsilon_{H_2O}$ : water dielectric constant;
- $\varepsilon_{Poly}$ : dry polyimide film dielectric constant;
- $\gamma_m$ : maximum fractional volume at  $T = 298\text{K}$  [15];
- $\phi(T)$ : temperature dependence on the adsorption coefficient;
- $\beta(T)$ : temperature dependence of the relative dielectric constant of water and the catalytic effect;

The temperature dependency of water with respect to temperature is expressed as [14], where  $T_0 = 298\text{K}$  (room temperature):

$$\varepsilon_{H_2O} = 78.54[1 - 4.6e^{-4}(T - T_0) + 8.8e^{-6}(T - T_0)^2] \quad (3)$$

From (1)(2)(3), the sensor front-end capacitance variation is both humidity and temperature dependent, which indicates that the sensitivity of the sensor would vary with ambient temperature. In this design, 500 $pst$  film from Dupont is selected for its high moisture absorption factor of 4% at 100%RH. At  $RH = 0\%$ ,  $\varepsilon_{500pst} = 3.9$  and  $\varepsilon_{H_2O} = 78.54$ .  $\gamma$  can

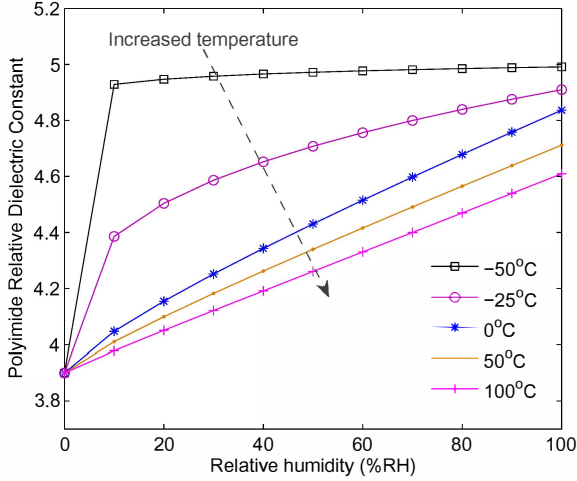


Fig. 2. Calculated polyimide relative dielectric constant relationship with ambient relative humidity and temperature.

be obtained from the validated parameters given in [16], calculated polyimide dielectric constant relationship with relative humidity from 0%RH to 100%RH and ambient temperature from  $-50^{\circ}\text{C}$  to  $100^{\circ}\text{C}$  is shown in Fig.2, Notice that, at low temperature, polyimide dielectric constant does not linearly change with relative humidity, another effect of the embedded heater is therefore to remain the sensor front-end at an optimal operation temperature.

Based on the capacitance modeling by [13][14][15], since  $C3$  is hidden from the polyimide film whose dielectric constant varies with relative humidity, the capacitance change of the front-end mainly depends on  $C1$  and  $C2$ , as shown in Fig.1. For a  $N$  finger array sensor, the total capacitance change with humidity can be expressed by:

$$\Delta C = (N - 1) \cdot (\Delta C1 + \Delta C2) \quad (4)$$

With  $\Delta\varepsilon_{Mix}$ , the total capacitance variation can be calculated as[15]:

$$\Delta C = (N - 1) \cdot \varepsilon_0 \cdot \Delta\varepsilon_{Mix} \cdot L \cdot \left[ \frac{m \cdot K(k')}{2 \cdot K(k)} + \frac{h}{W} \right] \quad (5)$$

where

$$m = 1 - e^{-2.2(\frac{H}{W+S})^2 - 3.9(\frac{H}{W+S})} \quad (6)$$

$$k = \sin\left[\pi \cdot \frac{W}{2(W+S)}\right]$$

$$k' = \cos\left[\pi \cdot \frac{W}{2(W+S)}\right]$$

And  $K(x)$  is the complete elliptic integral of the first kind.

As proved by other works, careful metal width and metal-to-metal gap selection can achieve even better sensitivity for the sensor front-end. This work trades the sensor sensitivity with chip area by adopting the minimum width and minimum metal pitch. For this work,  $N=40$ ,  $L = 175\mu\text{m}$ ,  $W = 2.5\mu\text{m}$ ,  $S = 2.6\mu\text{m}$ ,  $h = 0.99\mu\text{m}$  and  $H \approx 4.35\mu\text{m}$ . With the assist of above stated mathematical capacitance model, calculated

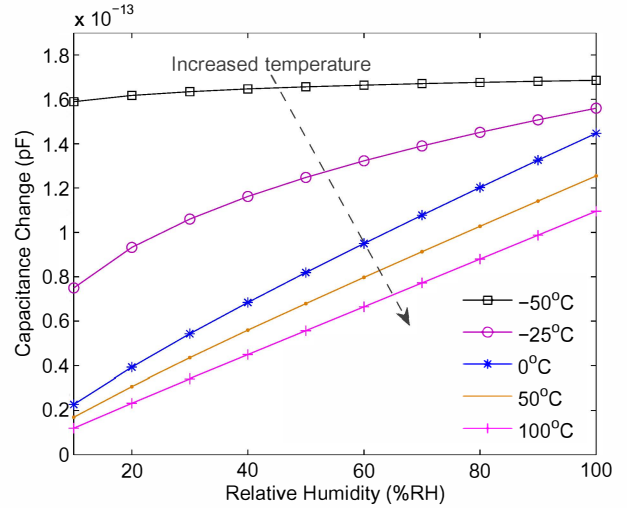


Fig. 3. Calculated capacitance change with ambient relative humidity and temperature for the designed sensor front-end.

capacitance change with respect to ambient relative humidity and temperature is shown in Fig.3.

As a result of chip area and sensitivity tradeoff, the designed front-end capacitor change with relative humidity is relatively weak, in the order of  $fF/\%RH$ . Dedicated readout scheme that is insensitive to device parasitic, wiring parasitic and absolute sensor capacitance and can amplify this capacitance difference is highly preferred.

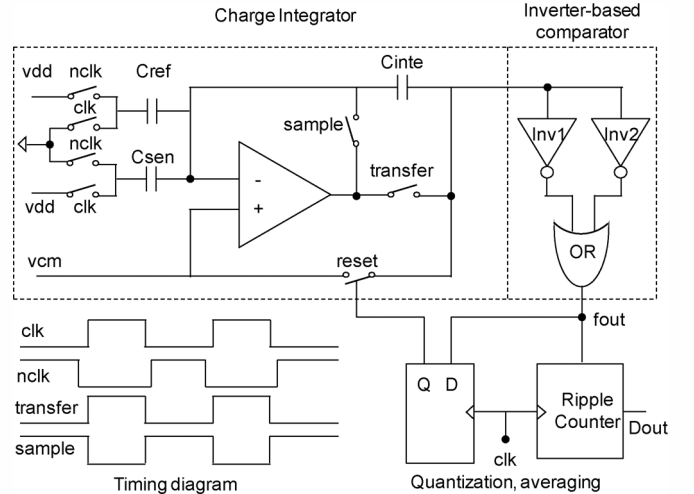


Fig. 4. Relative humidity sensor digital readout implementation and corresponding timing diagram

### C. Humidity Sensor Readout

Comparing with other works using high-cost sigma-delta ADC [6] or external  $\mu$ -controller [8] as the sensor readout, which are not suitable for miniaturized sensing platforms due to the high power consumption or high hardware complexity. This work adopts a modified first-order sigma-delta ADC [11] to achieve capacitance difference to digital conversion, which amplifies the capacitance difference and at the same

time averaging out circuit noise. Only one amplifier is needed for this converter core, much simpler and cheaper than other implementations. Fig.4 shows the implementation of the converter and its corresponding timing diagram.

The converter consists of three stages. The first stage is a voltage integrator, which consists of three capacitors and one high-gain amplifier.  $C_{sen}$  is the humidity sensor shown in Fig.1.  $C_{ref}$  is a reference capacitor which has the same structure with  $C_{sen}$  except that the filling material between the metal fingers is dielectric layer instead of polyimide.  $C_{ref}$  and  $C_{sen}$  are designed to have the same structure and routing paths to reduce their parasitic difference.  $C_{ref}$  and  $C_{sen}$  bottom plates are set at  $V_{cm}$  with a unit-gain feedback and their top plates are connected either to  $V_{dd}$  or  $V_{ss}$  based on the clock state. When  $clk$  is low, the amplifier is unit-gain configured by *sample*,  $C_{ref}$ 's top plate is connected to  $V_{dd}$  while  $C_{sen}$ 's to  $V_{ss}$ ; when  $clk$  is high, the amplifier is integrator configured by *transfer*,  $C_{ref}$ 's top plate is connected to  $V_{ss}$  while  $C_{sen}$ 's to  $V_{dd}$ , a charge amount of  $(C_{sen} - C_{ref}) \cdot V_{dd}$  is transferred to the integration capacitor  $C_{Inte}$ , with its voltage change of  $(C_{sen} - C_{ref}) \cdot V_{dd} / C_{Inte}$ . At the beginning of each conversion, capacitor  $C_{Inte}$  has to be reset by *reset*.

The second stage of the converter is a voltage to frequency converter, consisted by two inverters and one *or* gate. Transition threshold of the first inverter is designed to be  $V_{tri} = \frac{2}{3}V_{dd}$  and the second one is  $V_{tri} = \frac{1}{3}V_{dd}$  by adjusting PMOS/NMOS W/L ratio. If  $C_{sen} > C_{ref}$ , voltage of  $C_{Inte}$  will increase gradually from  $V_{cm}$  and trigger the  $f_{out}$  once  $V_{Inte} > \frac{2}{3}V_{dd}$ ; and vice versa if  $C_{sen} < C_{ref}$ . By doing so, the capacitance difference between  $C_{sen}$  and  $C_{ref}$  is amplified, thus increase the sensor resolution.  $f_{out}$  is reused to reset the integration capacitor and do multiple sampling to further average out circuit noise.

The third stage of the converter is a ripple counter that convert the capacitance difference into digital representation, as expressed by (7), where  $T$  is the time set for the counter and  $f$  is the sampling frequency and  $V_{cm}$  is set to half  $V_{dd}$ .

$$D = \frac{6T \cdot f \cdot (C_{sen} - C_{ref})}{C_{Inte}} = \frac{6T \cdot f \cdot (C_{sen0} + \Delta C_{sen} - C_{ref})}{C_{Inte}} \quad (7)$$

From(7), by matching the physical layout of  $C_{sen}$ ,  $C_{ref}$  and  $C_{Inte}$ , their capacitance ratio is only material dielectric constant dependent. As a consequence, after fabrication, the digital readout becomes a direct representation of ambient relative humidity, and its resolution can be improved by averaging more samples, namely, increase the sampling time  $T$ . In this design, the sampling frequency is set at 50kHz for less switching noise and the sampling time is 100ms for moderate sensing resolution and sampling rate.

### III. HUMIDITY SENSOR SIMULATION RESULTS

The sensor is designed in TSMC 0.18um process with thick top metal option. With the assist of dielectric constant and front-end capacitance modeling. The whole sensor system

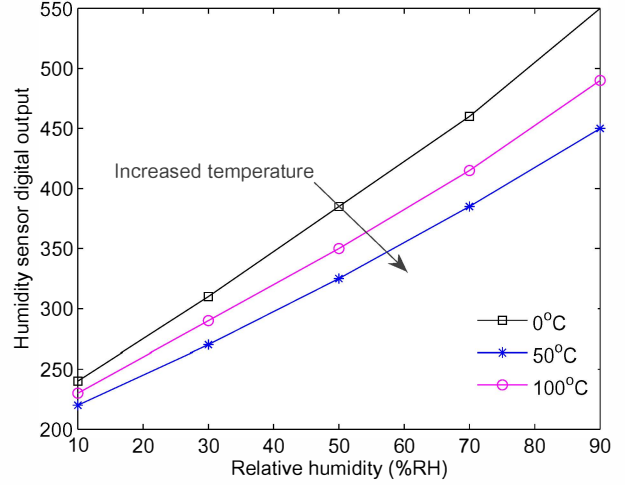


Fig. 5. Simulated digital output of the designed humidity sensor using modeled front-end capacitance change w.r.t. relative humidity.

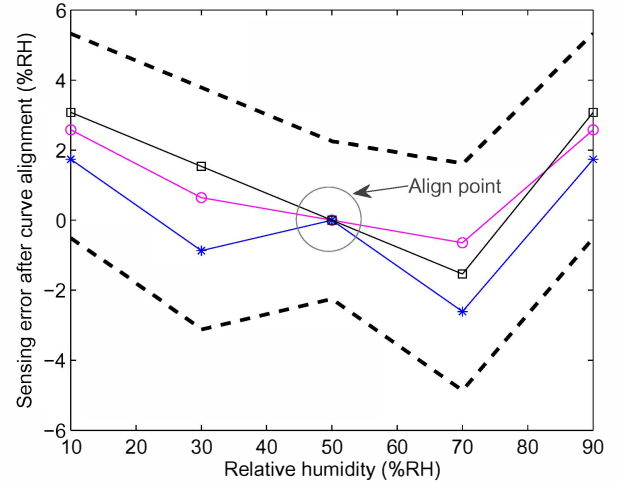


Fig. 6. Simulated sensor sensing inaccuracy w.r.t. relative humidity after linearization and data alignment, from 10%RH to 90%RH.

can be simulated combing the calculated capacitance and the readout circuitry. Fig.5 shows the digital output of the humidity sensor at different operating temperature. Fig.6 shows its non-linearity induced sensing error with respect to relative humidity. Process spread of this designed relative humidity sensor would be further checked during experimental testing. Since hysteresis effects cannot be simulated, based on several previous reported literatures, hysteresis induced sensing error is less than 2%RH if sensor heating is adopted during sensing. After adding this potential error source and a half-LSB sensing uncertainty, a sensing accuracy of +6/-5%RH can be expected from 10%RH to 90%RH, as shown in Fig.6.

At the same time, since the readout of the sensor is fully differential, time-degradation factor is almost the same for these three capacitors, it has the potential to maintain long-term stability. Fig.7 shows the micro-photograph of this sensor, which occupies a die area of 0.42mm<sup>2</sup>.

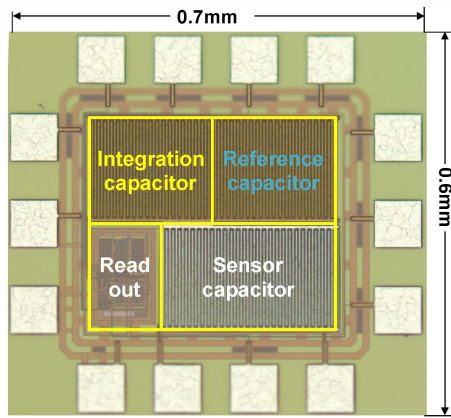


Fig. 7. Micro-photograph of the designed relative humidity sensor, occupying an area of  $0.42\text{mm}^2$ .

#### IV. CONCLUSION

A low-cost humidity sensor system is proposed in this work. Capacitance relationship of the sensing elements and the relative humidity is modeled and used in the sensor verification. A power efficient fully differential readout implementation ensures the parasitic immunity of the sensor and enable the sensor's long-term stable. An sensing inaccuracy of  $\pm 6/-5\%$ RH can be expected over a wide humidity range from 10%RH to 90%RH. This design is suitable for food monitoring applications, where a temperature sensor is generally attached, which can be utilized to further monitor the temperature sensitive relative humidity sensor.

#### REFERENCES

[1] Giorgio Sberveglieri; et al., "Characterization of porous  $\text{Al}_2\text{O}_3\text{-RSiO}_2/\text{Si}$  sensor for low and medium humidity ranges," *Sensors and Actuators B: Chemical*, vol.23, no. 2-3, pp.177-180, 1995.

[2] Baochang Cheng; et al., "Highly sensitive humidity sensor based on amorphous  $\text{Al}_2\text{O}_3$  nanotubes," *Journal of Materials Chemistry*, no. 6, pp.1907-1912, 2011.

[3] Zhi Chen; et al., "Humidity Sensors: A Review of Materials and Mechanisms," *Sensor Letters*, vol.3, pp.274295, 2005.

[4] Qin Kuang; et al., "High-Sensitivity Humidity Sensor Based on a Single  $\text{SnO}_2$  Nanowire," *Journal of the American Chemical Society*, vol.129, no. 19, pp.6070-6071, 2007.

[5] Seok-Ho Song; et al., "Metal-oxide-semiconductor field effect transistor humidity sensor using surface conductance," *Applied Physics Letters*, vol. 100, no. 10, 2012.

[6] Zhichao Tan; et al., "A 1.8V 11uW CMOS Smart Humidity Sensor for RFID Sensing Applications," *IEEE Asian Solid-State Circuits Conference*, pp.105-108, 2011.

[7] Lei Gu; et al., "A novel capacitive-type humidity sensor using CMOS fabrication technology," *Sensors and Actuators B: Chemical*, vol.99, no. 23, pp.491-498, 2004.

[8] Pelegri-Sebastian, J., "Low-Cost Capacitive Humidity Sensor for Application Within Flexible RFID Labels Based on Microcontroller Systems," *IEEE Transactions on Instrumentation and Measurement*, vol.61, no.2, pp.545-553, 2012.

[9] E. SACHER; et al., "Water Permeation of Polymer Films. I. Polyimide," *Materials and Engineering Analysis*, IBM Corporation.

[10] PETER J. SCHUBERT; et al., "Polyimide-Based Capacitive Humidity Sensor," *IEEE Transactions on Electron Devices*, vol.32, no.7, pp.1220-1223, 1985.

[11] Lee, H.; et al., "CMOS differential-capacitance-to-frequency converter utilising repetitive charge integration and charge conservation," *Electronics Letters*, vol.46, no.8, pp.567-569, 2010.

[12] Cheng-Long Zhao; et al., "A CMOS interdigital capacitive humidity sensor with polysilicon heaters," *IEEE Sensors Conference*, pp.382-385, 2010.

[13] N.J.Kidner; et al., "Modeling interdigital electrode structures for the dielectric characterization of electroceramic thin films," *Thin solid films*, vol.496, no.2, pp.539-545, 2006.

[14] Gevorgian, S.S.; et al., "CAD models for multilayered substrate interdigital capacitors," *Microwave Theory and Techniques*, vol.44, no.6, pp.896-904, 1996.

[15] Yang Wang; et al., "Modeling of a CMOS Capacitive Relative Humidity Sensor," *ETCS*, pp.209-212, 2009.

[16] Shibata, H.; et al., "A digital hygrometer using a polyimide film relative humidity sensor," *Instrumentation and Measurement*, vol.45, no.2, pp.564-569, 1996.